# **ProxMaP: Proximal Occupancy Map Prediction** for Efficient Indoor Robot Navigation

Vishnu D. Sharma

Jingxi Chen

Pratap Tokekar

Abstract—In a typical path planning pipeline for a ground robot, we build a map (e.g., an occupancy grid) of the environment as the robot moves around. While navigating indoors, a ground robot's knowledge about the environment may be limited due to occlusions. Therefore, the map will have many as-vet-unknown regions that may need to be avoided by a conservative planner. Instead, if a robot is able to correctly predict what its surroundings and occluded regions look like, the robot may be more efficient in navigation. In this work, we focus on predicting occupancy within the reachable distance of the robot to enable faster navigation and present a self-supervised proximity occupancy map prediction method, named ProxMaP. We show that ProxMaP generalizes well across realistic and real domains, and improves the robot navigation efficiency in simulation by 12.40% against the traditional navigation method. We share our findings on our project webpage.

#### I. Introduction

To navigate in a complex environment, a mobile robot needs to know the map of the environment. This information can either be provided as prior information by mapping the environment beforehand, or the robot can build a map in an online fashion using the sensors available to it. Occupancy maps are often used for this purpose, which provides probabilistic estimates about the free (navigable) and occupied (non-navigable) areas in the scene. These estimates can be updated as the robot gains more information about the environment during navigation.

Given an occupancy map, the robot can adjust its speed to navigate faster through high-confidence free and at a low speed through low-confidence, free areas so that it can stop before the collision. The navigation time thus depends on information regarding the map available to the robot. The obstacles in the environment pose the key hurdle here by occluding the robot's view. The problem is further exacerbated for sensors such as cameras that also have a limited field-of-view. These factors put a limit on the speed at which the robot could move through the environment.

In this paper, we train a neural network to predict occupancy in the regions that are currently occluded by obstacles, as shown in Figure 1. Prior works learn to predict the occupancy map all around the robot i.e., simulating a 360° field-of-view (Fov) given the visible occupancy map within a limited FoV only at the moment. Since the network is trained to predict the occupancy map all around the robot, it overfits by learning the room layouts. This happens as

This work is supported by the National Science Foundation under Grant No. 1943368 and ONR under grant number N00014-18-1-2829.

The authors are with the University of Maryland, College Park, USA {vishnuds, ianchen, tokekar}@umd.edu





robot in a living room

(a) Third-person view of the (b) Top view of the robot showing visibility polygon

Fig. 1: An example situation where the robot's view is limited by the obstacles (sofa blocking the view) and the camera field of view (sofa on the right is not fully visible).

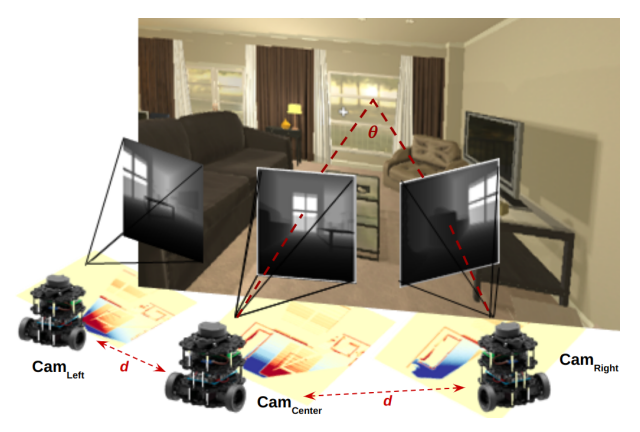
the network must learn to predict the occupancy information about the areas like the back of the robot, for which the robot may not have any overlapping information in its egocentric observations. This makes the prediction task difficult to learn. Furthermore, the ground truth requires mapping the whole scene beforehand, which could make sim-to-real transfer tedious. An additional challenge with this approach is that it requires mapping the whole environment in order to obtain the ground truth.

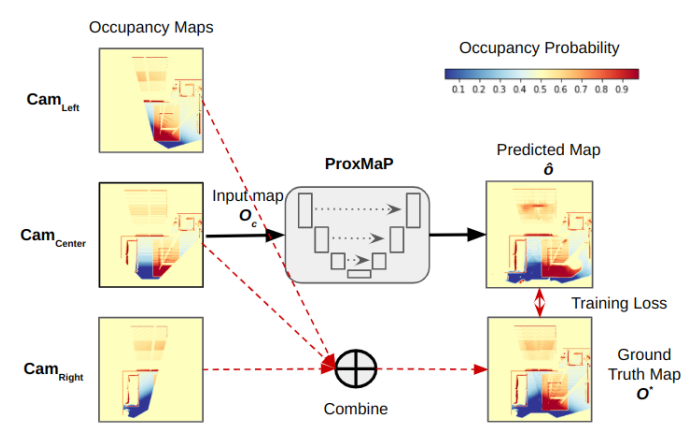
Our key insight is to simplify this problem by making predictions only about the proximity of the areas where the robot could move immediately. This setting has three-fold advantages: first, the prediction task is easier and relevant as the network needs to reason only about the immediately accessible regions (that are partly visible); second, the robot learns to predict obstacle shapes instead of learning room layouts, making it more generalizable; and third, ground truth is easier to obtain which can be obtained by moving the robot, making the approach self-supervised.

Following are our main contributions in this work:

- 1) We present ProxMaP, a self-supervised proximal occupancy map prediction method for indoor navigation, trained on occupancy maps generated from AI2THOR [1] simulator, and show that it makes accurate predictions and also generalizes well on HM3D dataset [2] without fine-tuning.
- 2) We study the effect of training ProxMaP under different paradigms on prediction quality and navigation tasks, highlighting the role of training methods on occupancy map prediction tasks. We also present some

<sup>1</sup> https://raaslab.org/projects/ProxMaP





(a) Movement configuration for data collection.

(b) Training and prediction overview.

Fig. 2: Overview of the proposed approach. The **training** and **inference** flows are indicated with red and black arrows, respectively. We take the input view by moving the robot to the left and right sides  $(Cam_{Left})$  and  $Cam_{Right}$ , looking towards the region of interest. ProxMaP makes predictions using the  $Cam_{Center}$  only, and the map obtained by combining the information from the three positions act as the ground truth.

- qualitative results on real data showing that ProxMaP can be extended to real-world inputs.
- 3) We simulate the point goal navigation as a downstream task utilizing our method for occupancy map prediction and show that our method outperforms the baseline, non-predictive approach, relatively by 12.40% in navigating faster, and even outperforms a robot with multiple cameras in the general setting.

#### II. RELATED WORK

Mapping the environment is a standard step for autonomous navigation. The mapping problem is coupled with the localization problem and is usually known as Simultaneous Localization and Mapping (SLAM) for which several classical algorithms exist [3], [4], [5]. The classical methods typically treat unobserved (i.e., occluded locations) as unknown. Our focus in this work is on learning to predict the occupancy values in these occluded areas. As shown by recent works, occupancy map prediction can help the robot navigate faster [6] and in an efficient manner [7].

Earlier works have explored machine learning techniques for occupancy map prediction [8], [9] targeted at online prediction, but they require updating the model online with new observations. Recent works have shifted to using neural networks for offline training to overcome this issue, treating the map-to-map prediction task as an inpainting problem. Katyal et al. [10] compare the efficacy of networks based on ResNet [11], UNet [12], [13] and GAN [14] for 2D occupancy map inpainting using LiDAR data, and show that UNet outperforms the others. Later works use UNet for occupancy map prediction with RGBD sensor and show improvement in robot navigation with the use of predicted maps [15], [16], [17] and extend this method to semantic information for further benefits [18].

Offline training for these methods requires ground truth collection by mapping the whole training environment. This

time-consuming process makes training and fine-tuning the models for new domains tedious, which also make real-world deployment difficult. Also, these models are trained to predict occupancy all around the robot, including the scene behind for which they may not have any context within the current observation, which could result in the networks memorizing room layouts, affecting their generalizability. Methods that rely on historical observations for predictions [19] also suffer from data efficiency challenges during training.

As robotic agents have the ability to actively collect data, self-supervised methods have been use successfully to address the data requirement issues for many robotic learning tasks [20], [21], [22], [23], [24]. In context of occupancy map prediction for robot indoor navigation, Wei et al. [25] proposed a self-supervised learning approach. They equip the robot with two RGB-D cameras at different heights, tilted toward the ground. A network is given the occupancy map from the lower camera and predicts the map resulting from the combined information from the two cameras. This approach is data-efficient, does not require manual annotation, and is shown to work well on real robots. This method is aimed at approaching the occupancy map behind the occlusion. But trained as a regression task, this method doesn't predict edge-like obstacles well and requires adding a camera to the robot for collecting data for finetuning. Lastly, tilted cameras limit the information about the scene ahead as compared to straight, forward-looking cameras.

To this end, we propose a self-supervised method consisting of a single, forward-looking camera, maximizing the information acquired about the navigation plane, while limiting the control effort required to collect data. The effort could be further minimized by adding two cameras to the side of the robot. We design our predictor as a classification network, which is able to generate sharper images compared

to the regression networks, as shown later in this work. We focus on making predictions in proximity of the robot, reducing the likelihood of memorization and and improving its generalizability by using the current view as context.

#### III. APPROACH

In this work, we consider a ground robot equipped with an RGBD camera in indoor environments. Two additional views are obtained by moving the robot around as shown in Figure 2a. In a real-world setting, this can also be adding extra cameras to the environment. In the following subsections, we detail the network architecture for ProxMaP, training details, and the data collection process.

# A. Network Architecture and Training Details

In our approach, we take the occupancy map generated by  $Cam_{Center}$  as input and generate an occupancy map with augmented information. Our goal is to accurately predict the occupancy information about the *unknown* cells in the input occupancy map. We use a neural network to achieve this and use the map generated by combining information from the three robot positions as the ground truth. Thus the network learns to predict the occupancy in its proximity.

We use a UNet architecture [12] for ProxMaP due to its ability to perform pixel-to-pixel prediction by sharing intermediate encodings with the decoder. Our network has a five-block encoder and a five-block decoder. For training, we convert these maps to 3-channel images representing *free*, *unknown*, and *occupied* regions. This is done by assigning each to one of the classes based on its probability p: if  $p \leq 0.495$ , the cells are treated as *free*; if  $p \geq 0.505$ , it is treated as *occupied*; and as *unknown* in rest of the cases. We train the network with cross-entropy loss, a popular choice for classification networks.

Since previous works have used variations of UNet for Occupancy map prediction training as a regression task [25], [20] and as a generative model [26], [6], we also train ProxMaP with these variations. We use UNet as the building block for these approaches as well with  $O_c$  as input and  $O^*$  as the target map (Figure 2b). For the regression tasks, these maps are transformed from log-odds to probability maps before training. For generative tasks, we use the UNet-based pix2pix [27] network with single-channel and three-channel input and output pairs for regression and classification, respectively.

For regression, since both input and output are probability maps, we use the KL-divergence loss function for training UNet, which simplifies to binary cross-entropy (BCE) under the assumption that each occupancy map is sampled from a multivariate Bernoulli distribution parameterized by the probability of each cell. In addition, we also train a UNet with Mean Squared Error (MSE) loss for regression.

For training the generative models, we use  $L_{L1}$  loss and  $L_{GAN}$  losses for generator G and discriminator D over input x and the target map y as defined below

$$\mathcal{L}_{L1}(G) = \mathbb{E}_x[\|y - G(x)\|_1] \tag{1}$$

$$\mathcal{L}_{GAN}(G, D) = \mathbb{E}_{y}[log D(y)] + \mathbb{E}_{x}[log(1 - D(G(x))]$$
 (2)

The training objective is to achieve a generator  $G^*$  such that

$$G^* = \arg\min_{G} \max_{D} \mathcal{L}_{GAN}(G, D) + \lambda \mathcal{L}_{L1}(G)$$
 (3)

In the rest of the discussion, while discussing ProxMaP's variations, we will refer to the generative classification, generative regression, and discriminative regression approaches as textitClass-GAN, *Reg-GAN*, and *Reg-UNet*, respectively.

#### B. Data Collection

We used AI2THOR [1] simulator which provides photorealistic scenes, corresponding depth and segmentation maps, and the flexibility to add multiple cameras to the environment. We add an RGBD camera, referred to as  $Cam_{Center}$ , at the height of 0.5m from the ground and at the same location as the robot. Two more observation are acquired by moving the robot, one towards the left  $(Cam_{Left})$  and the other towards the right side of the robot  $(Cam_{Right})$ , as shown in Figure 2a, at the same height h = 0.5m, but a distance d = 0.3m away horizontally from the original location. However, each camera is rotated by 30 deg from its principal axis to look toward the area directly in front of the robot. This is done to capture extra information about the scene, while also making sure that the cameras on the sides have some overlap with  $Cam_{Center}$  The rotation of the cameras virtually increases the field-of-view for the robot and the translation makes sure that the robot is able to learn to look around the corners rather than simply rotation at its location.

Each camera captures the depth image and the instance segmentation image. While the depth image helps with creating a 3D re-projection of the scene into point clouds, the latter helps with identifying the ceiling, which is excluded from the occupancy map generation process, and the floor, which acts as the free/navigable area. The rest acts as the occupied/non-navigable area for the robot. This segmentation-based processing step is used to process the information precisely and can be replaced with identifying the ceiling and floor using the height of the points after the re-projection. The point clouds are then projected back to the top-down view as we consider the problem of navigation on the 2D plane. For  $Cam_{Left}$  and  $Cam_{Right}$ , these views are first transformed from camera frame to robot-frame using rotation and translation. Then we limit the maps to the  $5m \times 5m$  area in front of the robot and convert them to  $256 \times 256$  images to use in the network. Each point belonging to the obstacles contributes to the addition of 1 point to the corresponding cell and the points for the floor contribute to the subtraction of 1 point. The number of points in each bin is multiplied with a factor m = 0.1 converting the map to an occupancy map with log odds. To prevent the map from having too large log-odds values, we clip the number of points in each to the range [-10, 10]. The resulting map from  $Cam_{Center}$ , referred to as  $O_c$ , acts as the input to the network. Similar to Wei et al. [25], we construct the ground truth map  $O^*$ , as the combination of the maps from the three cameras as follows:

$$O^* = max\{abs(O_c), abs(O_l), abs(O_r)\} \cdot sign(O_c + O_l + O_r)$$
(4)

where  $O_c$ ,  $O_l$  and  $O_r$  refer to the occupancy maps generated by  $Cam_{Center}$ ,  $Cam_{Left}$ , and  $Cam_{Right}$ , respectively. These log-odds maps are converted to probability maps before being used for network training.

AI2THOR provides different types of rooms. We use living rooms only as they have a larger size and contain more obstacles compared to others. Out of the 30 such rooms, we use the first 20 for training and validation and the rest for testing. For data collection, we divide the floor into square grids of size 0.5m and rotate the cameras by  $360^{\circ}$  in steps of  $45^{\circ}$ . As some maps do not contain a lot of information to predict due to the robot being closed to the walls, we filter out the pairs of the map where the number of occupied cells in  $O^*$  is more than 20%. This process provides us with  $\sim 6000$  map pairs for training and  $\sim 2000$  pairs for testing.

#### IV. EXPERIMENTS & RESULTS

We report two types of results in this section. First, we present the prediction performance of the ProxMaP and its variations on our test dataset from AI2THOR. Additionally, we show prediction results on HM3D [2] to test generalizability. Then we use these networks for indoor point-goal navigation and compare with non-predictive methods and state-of-the-art self-supervised approach (Wei et al. [25]). Finally, we show some qualitative results on a few real observations to highlight the potential of real-world applications. The networks were trained on a GeForce RTX 2080 GPU, with a batch size of 4 for GANs and 16 for discriminative models. Early stopping was used to avoid overfitting the network with the maximum number of epochs set to 300.  $\lambda$  was set to 100 for training GANs.

# A. Occupancy Map Prediction

**Setup:** Since our ground truth maps are generated from a limited set of observations, they may not contain the occupancy information of all the surrounding cells. Hence, we evaluate the predictions only predictions in cells whose ground truth occupancy is known to be either occupied or free. We refer to such cells as *inpainted cells*. For the classification task, we choose the most likely label as the output for each cell. For regression networks, a cell is considered to be *free* if the probability p in this cell is lesser than 0.495. Similarly, a cell with  $p \geq 0.505$  is considered to be *occupied*. The remaining cells are treated as *unknown* and are not considered in the evaluations.

Prediction accuracy is a typical metric to evaluate the prediction quality. However, it may not present a clear picture of our situation due to the data imbalance caused by fewer occupied cells. Ground robots with cameras at low heights, similar to our case, are more prone to data imbalance as the robot may only observe the edges of the obstacles. Thus we also present the precision, recall, and F-score for each class.

**Results:** Figure 3 show the qualitative results of ProxMaP and its variants and summarize the quantitative results in Table I. We found that classification networks, ProxMaP in particular, are better at predicting occupied cells precisely. Regression networks, on the other hand, tend to predict the areas surrounding the observed occupied cells as occupied, which is likely to be an obstacle in reality and thus yield a higher recall than the classification networks. This difference is evident in the prediction of the left edge of the sofa on top in Example 1 (Figure 3). ProxMaP, owing to a wider gap in precision with respect to the regression networks, has a higher F-score. The generative networks fell behind here because during the training they tend to learn the patterns too closely, including the patterns for unknown cells. This can be seen in prediction in the bottom right corner of the room in Example 3, where both Reg-GAN and Class-GAN try to mimic the locations of the unknown cells in the ground truth. In the regression task, MSE loss is also better than BCE, which tends to diffuse the observed cells and thus does not perform as well as MSE loss.

Generalizability: We test the generalizability of ProxMaP prediction over ~5000 map pairs obtained from HM3D dataset [2] which comprises of sensor data from a realistic setting, in a manner similar to the one used for AI2THOR. We find the same metrics as the previous experiment and summarize the results in Table II. We observe that the discriminative regression models exhibit higher accuracy than other models, but the other metrics follow a similar pattern as earlier, i.e. ProxMaP leading across the F1-score and precision for the known classes. We note that all the metrics are lower than the results on AI2THOR (Table I) due to the difference in the data sources, as expected.

To summarize, classification networks are better than regression for occupancy prediction with higher accuracy and F-score. Generative approaches work better at classification than regression but one should be careful in using them as they tend to learn all patterns in the ground truth, including the undesirable ones. We present more qualitative results on our project webpage.

## B. Navigation Performance

Setup: We use the occupancy map prediction network for point-goal navigation in an unknown environment by repeated prediction and planning over the path. We also compare the discriminative and generative variation here and use only Reg-UNet(MSE) as the discriminative regression method as it performs better than Reg-UNet(BCE). We compare these methods against an approach relying solely on the input map  $O_c$ , which we refer to as the baseline, and the method proposed by Wei et al. [25], but trained with MSE loss instead of BCE as the network trained with BCE loss (proposed by the authors) did not perform well. We obtained an F1-score of 44.01% with BCE loss as compared to the F1-score of 47.61% for the network trained with MSE loss. Additionally, we compare these methods against the setting where the robot is equipped with cameras on the side as well, i.e., when  $Cam_{Left}$  and  $Cam_{Right}$  directly provide

TABLE I: Comparison across different variations of ProxMaP over living room data from AI2THOR [1] simulator. Abbreviations *Reg* and *Class* refer to *Regression* and *Classification* tasks, respectively

Method	F1-Score			Precision			Recall			
	Free	Unknown	Occupied	Free	Unknown	Occupied	Free	Unknown	Occupied	Accuracy
Reg-UNet (MSE)	82.09%	90.39%	67.08%	73.91%	96.31%	60.28%	92.32%	85.15%	75.62%	90.94%
Reg-UNet (BCE)	81.37%	89.53%	65.08%	72.03%	96.76%	57.49%	93.51%	83.30%	74.99%	90.85%
Reg-GAN	77.90%	91.14%	67.51%	81.78%	89.57%	69.19%	74.38%	92.77%	65.91%	86.92%
Class-GAN	82.86%	93.08%	72.22%	82.58%	92.32%	81.14%	83.14%	93.85%	65.07%	89.71%
ProxMaP	85.43%	94.19%	76.12%	87.42%	92.38%	88.07%	83.52%	96.07%	67.02%	92.44%

TABLE II: Generalizability of ProxMaP and variations over Habitat-Matterport3D (HM3D) [2] dataset. Abbreviations *Reg* and *Class* refer to *Regression* and *Classification* tasks, respectively

Method	F1-Score			Precision			Recall			
	Free	Unknown	Occupied	Free	Unknown	Occupied	Free	Unknown	Occupied	Accuracy
Reg-UNet (MSE)	79.99%	85.91%	56.33%	72.24%	93.52%	44.48%	89.59%	79.45%	76.79%	90.08%
Reg-UNet (BCE)	78.70%	84.40%	49.92%	69.70%	94.84%	36.96%	90.37%	76.02%	76.91%	90.81%
Reg-GAN	75.05%	88.25%	56.21%	82.38%	85.42%	51.17%	68.92%	91.28%	62.36%	83.55%
Class-GAN	80.27%	90.04%	70.81%	81.65%	89.04%	76.01%	78.93%	91.05%	66.28%	86.41%
ProxMaP	81.50%	90.91%	74.11%	84.32%	89.07%	84.22%	78.86%	92.83%	66.16%	87.54%

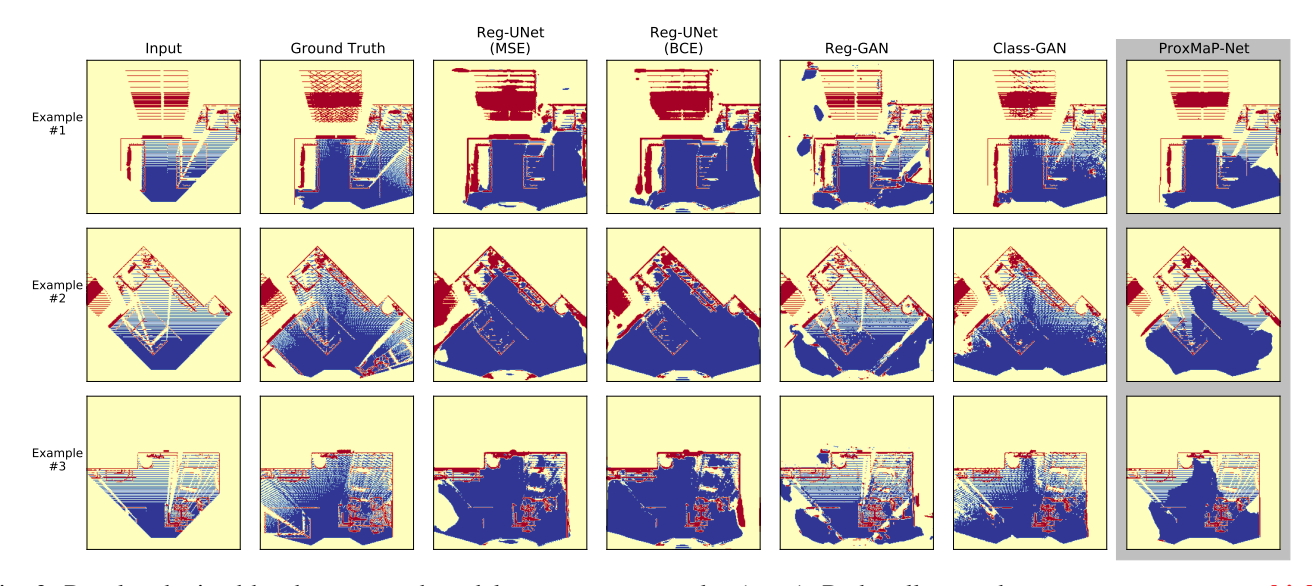


Fig. 3: Results obtained by the proposed model over some examples (rows). Red, yellow, and green areas represent a high, moderate, and low chance of occupancy in an area. ProxMaP makes more accurate and precise predictions than others.

the inputs (thereby not requiring any prediction) about the scene (referred to as 3-Cameras).

In each trial, we first randomly generate a start location, a destination, and initial yaw for the robot. At each step, the robot generates an occupancy map using the RGB-D camera. The robot also keeps a global occupancy map in the memory. We use the perceived height to filter out the ceiling and other obstacles situated at a height higher than the robot, rather than using the ground truth semantic maps for filtering. We assume that the robot knows its global location and yaw without error. An augmentation method, described below, modifies the occupancy map and updates its global

map using the same method as used for the ground truth generation (Eq. 4). This global map is transformed into a cost map for the path planner. The path planner uses Dijkstra's algorithm to find the shortest path to the destination. The robot then navigates to the next waypoint prescribed by the planner, moving in the steps of 20cm, if it is within 1° of the robot's line of sight. Otherwise, the robot rotates to face the waypoint and then moves. The room is discretized into a grid of square cells with sides 0.2m. The simulation ends either if the goal is within one diagonal cell at most, or if the robot has moved and rotated  $S_{max}$ =100 times, which we found is enough to reach the goal unless the robot gets stuck.

TABLE III: SCT performance across different living rooms

Method	SCT
Baseline (no prediction)	0.589
Wei et al. [25] (MSE)	0.568
Reg-UNet (MSE)	0.629
Reg-GAN	0.592
Class-GAN	0.632
ProxMaP	0.662
3-Cameras (no prediction)	0.648

For path planning, the sensed occupied and free areas are given preference over the predicted counterparts in the maps, and the costs are accordingly weighted in the cost maps.

We keep the speed of the robot proportional to its confidence about the free cells on the predicted path. Thus the robot moves faster when it is confident about not colliding with an obstacle on the path. If there are possible obstacles on the path, it should keep its speed lower to be able to stop before a collision. The cost of the traversal is equal to the time taken to reach the goal.

To measure the navigation efficiency in terms of time, we use *Success weighted by (normalized inverse) Completion Time* [28] as the metric, which is defined as follows:

$$SCT = \frac{1}{N} \sum_{i=1}^{N} S_i \frac{l_i}{max(p_i, l_i)}$$
 (5)

where, N is the number of test episodes,  $S_i$  a binary variable indicating success in the  $i^{th}$  episode,  $l_i$  is the traversal time on the shortest path between the source and destination and  $p_i$  is the measured traversal time by the robot in this episode. In our case,  $S_i$  is 1 only when the robot is within one cell away, the number of total steps does not exceed  $S_{max}$ , and the simulator does not run into an error during simulation. Here,  $l_i$  is found by running a simulation on the global map generated using the reachable positions at the start of the simulations. This map does not depend on sensing and thus is not updated during an episode. Here,  $p_i$  is calculated as the time taken for traversal by the robot. A higher value of SCT indicates a higher success rate and  $p_i$  being closer to  $l_i$ . Thus, a method with higher SCT is preferred.

First, we compare the navigation efficiency by simulating navigation in different living rooms (FloorPlan221-227). We report SCT over N=102 episodes in these rooms in Table III. Most of these rooms are smaller and have fewer situations where the robot needs to choose between multiple paths. We observe that the classification models outperform the others, reaching a maximum relative benefit of 12.39% against the baseline approach. ProxMaP even outperforms the 3-cameras method by a relative margin of 2.16%. We found that this happens because the prediction can also fill the gaps in the map that the 3-camera setup can not observe and hence results in higher navigation speed over the path. The prediction method by Wei et al. [25], which relies on a higher-lower camera setup, fails to outperform the baseline in this situation. Other variations of ProxMaP also outperform

the baseline, highlighting the benefit of making predictions in proximity. These variations however fall short in comparison to the 3-camera setup.

To study the navigation performance in a more complex situation with a higher emphasis on decision-making, we use a modified version of the living room FloorPlan227 due to its larger size and higher number of obstacles, and therefore, more possible paths to the goals. We remove an armchair to allow the robot more choices in terms of paths. We find that over N=100 episodes in the modified FloorPlan227 environment. ProxMaP achieves a relative improvement in SCT by 8.62% over the Baseline and 7.2% improvement over Wei et al. [25]. In many cases, an erroneous prediction may discourage the robot from moving on a shorter path to the goal, resulting in longer navigation time. We present a summary of these results on our project webpage.

In summary, in the navigation tasks, classification approaches perform relatively better, similar to the prediction performance, suggesting they are more suitable for occupancy map prediction. They are also more generalizable and precise, both as an individual predictor and in conjunction with the navigation planner.

## C. Predictions on Real Data

For testing ProxMaP on real data, we use a TurtleBot2 robot equipped with a Hokuyo 2D laser scanner. We limit the field of view of the scanner to  $45^{\circ}$  and use its reading to generate the occupancy maps. We use ProxMaP over this map to make predictions. Figure 4 shows the third-person view of the robot in an artificial maze created in our lab and the qualitative results for some interesting situations. In these maps, the unknown, free, and occupied regions are shown in green, blue, and red, respectively. Similar to our training conditions, the scanner at a low height can only observe the edges of the obstacles. In these situations, we show that even when a part of the obstacle is visible, ProxMaP is able to estimate its shape very well, while also predicting the nearby free regions. We perform these predictions offline due to the prediction latency but will explore the real-time deep learning libraries in future work.

## V. CONCLUSION

In this paper, we proposed ProxMaP, a self-supervised method for the occupancy map prediction in the robot's proximity to aid robot navigation in presence of obstacles in the scene. We showed that our method is more precise in its predictions, is generalizable over realistic and real inputs, and outperforms other approaches to improve robot navigation time by varying the robot speed based on the observed and predicted information. We also find the ProxMaP has the potential to outperform the equivalent multi-camera setup.

We also study different variations of ProxMaP and show that the classification approaches result in better predictions, both qualitatively and quantitatively, compared to the regression-based approaches, and help the robot navigate faster by making inferences about the nearby regions occluded by the obstacles. While generative approaches provide

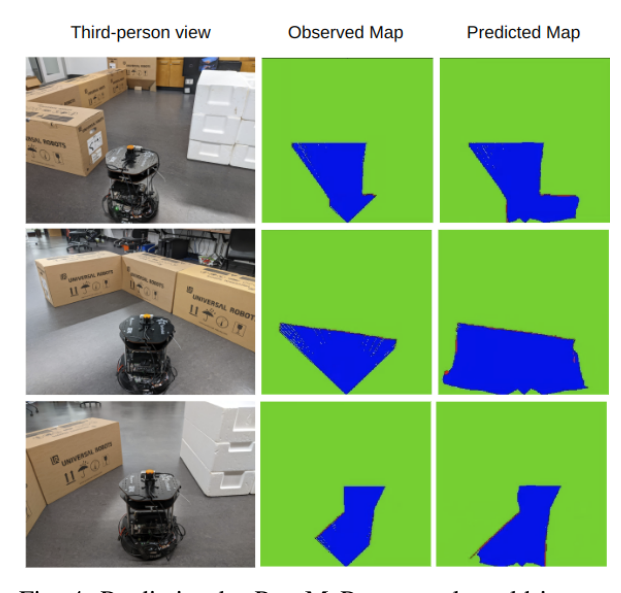


Fig. 4: Prediction by ProxMaP over real-world inputs.

promising alternatives, they may learn undesired patterns from the data and should be used with caution.

The proposed method can be further extended to study the effect of different placements of  $Cam_{Left}$  and  $Cam_{Right}$  on robot navigation. The method may also benefit from leveraging other sensor and input modalities for prediction and planning. Our preliminary studies on including semantic information show encouraging results and will be explored in future work.

#### REFERENCES

- E. Kolve, R. Mottaghi, W. Han, E. VanderBilt, L. Weihs, A. Herrasti,
   D. Gordon, Y. Zhu, A. Gupta, and A. Farhadi, "Ai2-thor: An interactive 3d environment for visual ai," arXiv preprint arXiv:1712.05474, 2017.
- [2] S. K. Ramakrishnan, A. Gokaslan, E. Wijmans, O. Maksymets, A. Clegg, J. M. Turner, E. Undersander, W. Galuba, A. Westbury, A. X. Chang, M. Savva, Y. Zhao, and D. Batra, "Habitat-matterport 3d dataset (HM3d): 1000 large-scale 3d environments for embodied AI," in Thirty-fifth Conference on Neural Information Processing Systems Datasets and Benchmarks Track (Round 2), 2021. [Online]. Available: https://openreview.net/forum?id=-v4OuqNs5P
- [3] G. Grisetti, C. Stachniss, and W. Burgard, "Improved techniques for grid mapping with rao-blackwellized particle filters," *IEEE Transac*tions on Robotics, vol. 23, no. 1, pp. 34–46, 2007.
- [4] W. Hess, D. Kohler, H. Rapp, and D. Andor, "Real-time loop closure in 2d lidar slam," in 2016 IEEE International Conference on Robotics and Automation (ICRA), 2016, pp. 1271–1278.
- [5] A. Hornung, K. M. Wurm, M. Bennewitz, C. Stachniss, and W. Burgard, "Octomap: An efficient probabilistic 3d mapping framework based on octrees," *Autonomous robots*, vol. 34, no. 3, pp. 189–206, 2013.
- [6] K. D. Katyal, A. Polevoy, J. Moore, C. Knuth, and K. M. Popek, "High-speed robot navigation using predicted occupancy maps," in 2021 IEEE International Conference on Robotics and Automation (ICRA). IEEE, 2021, pp. 5476–5482.
- [7] A. Elhafsi, B. Ivanovic, L. Janson, and M. Pavone, "Map-predictive motion planning in unknown environments," in 2020 IEEE International Conference on Robotics and Automation (ICRA). IEEE, 2020, pp. 8552–8558.
- [8] S. T. O'Callaghan and F. T. Ramos, "Gaussian process occupancy maps," *The International Journal of Robotics Research*, vol. 31, no. 1, pp. 42–62, 2012.

- [9] K. Doherty, J. Wang, and B. Englot, "Bayesian generalized kernel inference for occupancy map prediction," in 2017 IEEE International Conference on Robotics and Automation (ICRA), 2017, pp. 3118– 3124.
- [10] K. Katyal, K. Popek, C. Paxton, J. Moore, K. Wolfe, P. Burlina, and G. D. Hager, "Occupancy map prediction using generative and fully convolutional networks for robot navigation," arXiv preprint arXiv:1803.02007, 2018.
- [11] K. He, X. Zhang, S. Ren, and J. Sun, "Deep residual learning for image recognition, corr abs/1512.03385 (2015)," 2015.
- [12] O. Ronneberger, P. Fischer, and T. Brox, "U-net: Convolutional networks for biomedical image segmentation," in *International Confer*ence on Medical image computing and computer-assisted intervention. Springer, 2015, pp. 234–241.
- [13] Y. Katsumata, A. Kanechika, A. Taniguchi, L. El Hafi, Y. Hagiwara, and T. Taniguchi, "Map completion from partial observation using the global structure of multiple environmental maps," *Advanced Robotics*, vol. 36, no. 5-6, pp. 279–290, 2022.
- [14] I. Goodfellow, J. Pouget-Abadie, M. Mirza, B. Xu, D. Warde-Farley, S. Ozair, A. Courville, and Y. Bengio, "Generative adversarial nets," *Advances in neural information processing systems*, vol. 27, 2014.
- [15] S. K. Ramakrishnan, Z. Al-Halah, and K. Grauman, "Occupancy anticipation for efficient exploration and navigation," in *European Conference on Computer Vision*. Springer, 2020, pp. 400–418.
- [16] G. Georgakis, B. Bucher, K. Schmeckpeper, S. Singh, and K. Daniilidis, "Learning to map for active semantic goal navigation," arXiv preprint arXiv:2106.15648, 2021.
- [17] G. Georgakis, B. Bucher, A. Arapin, K. Schmeckpeper, N. Matni, and K. Daniilidis, "Uncertainty-driven planner for exploration and navigation," arXiv preprint arXiv:2202.11907, 2022.
- [18] G. Georgakis, K. Schmeckpeper, K. Wanchoo, S. Dan, E. Miltsakaki, D. Roth, and K. Daniilidis, "Cross-modal map learning for vision and language navigation," in 2022 IEEE/CVF Conference on Computer Vision and Pattern Recognition (CVPR), 2022, pp. 15439–15449.
- [19] L. Rummelhard, A. Negre, and C. Laugier, "Conditional monte carlo dense occupancy tracker," in 2015 IEEE 18th International Conference on Intelligent Transportation Systems. IEEE, 2015, pp. 2485–2490.
- [20] M. Stölzle, T. Miki, L. Gerdes, M. Azkarate, and M. Hutter, "Reconstructing occluded elevation information in terrain maps with self-supervised learning," *IEEE Robotics and Automation Letters*, vol. 7, no. 2, pp. 1697–1704, 2022.
- [21] P. Hu, A. Huang, J. Dolan, D. Held, and D. Ramanan, "Safe local motion planning with self-supervised freespace forecasting," in *Pro*ceedings of the IEEE/CVF Conference on Computer Vision and Pattern Recognition, 2021, pp. 12732–12741.
- [22] T. Khurana, P. Hu, A. Dave, J. Ziglar, D. Held, and D. Ramanan, "Differentiable raycasting for self-supervised occupancy forecasting," in Computer Vision–ECCV 2022: 17th European Conference, Tel Aviv, Israel, October 23–27, 2022, Proceedings, Part XXXVIII. Springer, 2022, pp. 353–369.
- [23] H. Wang, Y. Sun, Q. J. Wu, X. Lu, X. Wang, and Z. Zhang, "Self-supervised monocular depth estimation with direct methods," *Neurocomputing*, vol. 421, pp. 340–348, 2021. [Online]. Available: https://www.sciencedirect.com/science/article/pii/ S0925231220315599
- [24] L. Wellhausen, A. Dosovitskiy, R. Ranftl, K. Walas, C. Cadena, and M. Hutter, "Where should i walk? predicting terrain properties from images via self-supervised learning," *IEEE Robotics and Automation Letters*, vol. 4, no. 2, pp. 1509–1516, 2019.
- [25] M. Wei, D. Lee, V. Isler, and D. Lee, "Occupancy map inpainting for online robot navigation," in 2021 IEEE International Conference on Robotics and Automation (ICRA). IEEE, 2021, pp. 8551–8557.
- [26] K. Katyal, K. Popek, C. Paxton, P. Burlina, and G. D. Hager, "Uncertainty-aware occupancy map prediction using generative networks for robot navigation," in 2019 International Conference on Robotics and Automation (ICRA). IEEE, 2019, pp. 5453–5459.
- [27] P. Isola, J.-Y. Zhu, T. Zhou, and A. A. Efros, "Image-to-image translation with conditional adversarial networks," in *Proceedings of* the IEEE conference on computer vision and pattern recognition, 2017, pp. 1125–1134.
- [28] N. Yokoyama, S. Ha, and D. Batra, "Success weighted by completion time: A dynamics-aware evaluation criteria for embodied navigation," in 2021 IEEE/RSJ International Conference on Intelligent Robots and Systems (IROS). IEEE, 2021, pp. 1562–1569.